ARTICLE OPEN

Check for updates

mPFC DCC coupling with CaMKII$^+$ neuronal excitation participates in behavioral despair in male mice

Ping Cheng[1,3], Keke Ding[1,3], Daokang Chen[1,3], Chen Yang[1], Juan Wang[1], Shaojie Yang[1], Ming Chen[2✉] and Guoqi Zhu[1✉]

A longed lack of control over harmful stimuli can lead to learned helplessness (LH), a significant factor in depression. However, the cellular and molecular mechanisms underlying LH, and eventually behavioral despair, remain largely unknown. The *deleted in colorectal cancer* (*dcc*) gene is associated with the risk of depression. However, the therapeutic potential and regulation mechanism of DCC in behavioral despair are still uncertain. In this study, we showed that depressive stimulators, including LH, lipopolysaccharide, and unpredictable chronic mild stress, triggered an elevation in DCC expression in the medial prefrontal cortex (mPFC). Additionally, elevated DCC expression in the mPFC was crucial in inducing behavioral despair, as evidenced by the induction of behavioral despair in normal mice and exacerbation of behavioral despair in LH mice upon DCC overexpression. By contrast, neutralizing DCC activity ameliorated LH-induced behavioral despair. Importantly, we elucidated that pathological DCC expression was attributable to the excessive excitation of CaMKII$^+$ neurons in a manner dependent on the calpain-mediated degradation of SCOP and aberrant phosphorylation of the ERK signaling pathway. In addition, the increase in DCC expression led to a decreased excitability threshold in CaMKII$^+$ neurons in the mPFC, which was supported by the observation that the ligand netrin 1 increased the frequency of action potential firing and of spontaneous excitatory postsynaptic currents in CaMKII$^+$ neurons. In conclusion, our data indicate that LH triggers the excessive excitation of CaMKII$^+$ neurons and activation of calpain-SCOP/ERK signaling to promote DCC expression, and DCC represents a crucial target for the treatment of LH-induced behavioral despair in male mice.

Translational Psychiatry (2025)15:52 ; https://doi.org/10.1038/s41398-025-03266-x

INTRODUCTION

Depression is one of the most common neuropsychiatric disorders. Its main symptoms are characterized by a persistent low mood and lack of pleasure, often accompanied by sleep disorders and abnormal appetite, and can even lead to suicide in severe cases [1–5]. With the COVID-19 pandemic, the incidence of depression has increased significantly [6–8]. At present, the mechanisms of depression are still unclear, and clinically, difficulties occur with using medications for the condition, such as poor adherence, low efficiency, slow onset of action, and high relapse rates after discontinuation. A lack of control over harmful stimuli may lead to learned helplessness (LH), which is similar to depression and post-traumatic stress disorder in the symptoms. In chronic pain and cancer patients especially, the psychological stress caused by LH can exacerbate pain or even enhance tumor growth [9]. However, only a few molecular targets in the brain that are involved in the process of psychological stress-induced depression have been revealed.

The deleted in colorectal cancer (DCC) interacts with the classical axon guidance molecule netrin 1 (NT-1) to mediate neuronal axon growth, and DCC plays pivotal roles in neurogenesis, the morphogenesis of neuronal structures, as well as neural circuit formation [10–13]. Reportedly, the aberrant expression of DCC and its ligand NT-1 are involved in a variety of neuropsychiatric disorders, including brain injury [14] and schizophrenia [15]. A research team demonstrated that *dcc* is a risk gene for depression and multiple allele genotypes related to depression risk are associated with high DCC expression in the medial prefrontal cortex (mPFC) [16, 17]. Additionally, experimental evidence suggested that the miR-218 regulation of DCC expression participated in depression or depression-like syndrome in a chronic social defeat stress mouse model [18, 19]. There have been no further updates on research into the role of DCC, leaving the therapeutic potential and regulation mechanism of DCC still uncertain.

The mPFC and its associated neural circuits play an important role in the pathophysiology of depression. Research has shown that stress causes changes in neuronal activity, leading to either excitation or inhibition in the mPFC [20–22]. Generally, disturbances in the excitatory/inhibitory network of the mPFC have been deemed important for the development of depression-like syndrome, and chronic stress is thought to trigger excessive neuronal excitement and disturb the balance between excitement and inhibition [23]. However, the molecular mechanisms underlying impaired neuronal function in the mPFC and the pathogenesis of depression-like syndrome are still unknown. Calpain is a

[1]Center for Xin'an Medicine and Modernization of Traditional Chinese Medicine of IHM, and Key Laboratory of Molecular Biology (Brain diseases), Anhui University of Chinese Medicine, Hefei, China. [2]MOE Frontier Center for Brain Science, Institutes of Brain Science, State Key Laboratory of Medical Neurobiology, Fudan University, Shanghai, China. [3]These authors contributed equally: Ping Cheng, Keke Ding, Daokang Chen. ✉email: ming_chen@fudan.edu.cn; guoqizhu@gmail.com

Received: 27 May 2024 Revised: 13 January 2025 Accepted: 30 January 2025
Published online: 14 February 2025

member of a class of Ca^{2+}-dependent cysteine proteases that can be activated by high concentrations of Ca^{2+} and is essential for controlling the activation state of neurons. The excessive activation of calpain is involved in the development of metabolic diseases and cardiac diseases [24, 25], neurodegenerative diseases [26, 27], and depression-like syndrome [28]. Given that calpain plays a crucial role in initiating neuronal excitability, it is possible that it is involved in the regulation of impaired neuronal function in the mPFC and thus mediates the onset of depression.

In this study, we applied LH stress in an animal model and focused on investigating the role of mPFC DCC in LH and LH-induced behavioral despair, an important feature of depression-like syndrome in male mice. Therapeutic targets of DCC were investigated using the lentiviral overexpression of DCC, a DCC-neutralizing antibody, and the classical rapid antidepressant ketamine. Later, pathological DCC expression was investigated from the perspective of neuronal excitation and related signaling pathways. Finally, the effects of DCC on $CaMKII^{+}$ neuronal excitation were further investigated. The findings of study suggest that DCC is a potential target for the treatment of LH-induced behavioral despair in male mice.

MATERIALS AND METHODS

Animals and groups

All experimental animals used in this study were 8- to 10-week old male C57BL/6 mice provided by the Experimental Animal Center of Anhui Medical University. The mice were housed in groups of four in cages kept at a stable temperature and humidity (ambient temperature: 22 ± 2 °C, humidity 45–65%), and light cycle (8:00 am to 8:00 pm), unlimited water and food supplies, and good ventilation. Animals were acclimatized and fed for one week prior to the experiments, and all animal experiments in this study were complied with National Institutes of Health (NIH) guidelines for the Care and Use of Laboratory Animals and approved by the Animal Ethics Committee of Anhui University of Chinese Medicine (AHUCM-mouse-2022014).

The animals used in each experiment were randomly assigned to each group and the investigators were blinded to the group allocation during the experiments. According to the preliminary experimental results, the number of animals required to achieve significant behavioral differences is no fewer than 5. In line with the principle of reducing animal usage and considering the relative stability of biochemical and staining experiments, each group in these experiments consisted of 3 or 4 animals, with each animal's experiment being repeated at least 3 times to obtain an average value. The details of the N values have been included in the figure legends.

Preparation of animal models

Learned helplessness. The method used for recreating the LH model was as described previously [29]. After 1 week of acclimatization, mice in the model group were given unavoidable plantar electric shocks (stimulus current strength of 0.8 mA, 20 s per shock, 10 s interval) 30 times in a shock box for 3 consecutive days, and mice in the control group were placed in the same environment without plantar shocks. After a sustained period of time under uncontrollable and unavoidable stress, the animals eventually developed behavioral despair, as evidenced by their lack of stimulus avoidance and interference of subsequent adaptive responses. Behavioral tests were performed 24 h later.

Lipopolysaccharide (LPS)-induced mouse model. LPS is an inflammatory substance that can cross the blood-brain barrier after intraperitoneal injection and induce an inflammation model of depression [30]. After one week of adaptation, mice in the model group were given intraperitoneal injections of LPS (Sigma, L2630) at a dose of 2 mg/kg. LPS was dissolved in saline, and the mice in the normal control group were given intraperitoneal injections of saline.

Unpredictable chronic mild stress. The unpredictable chronic mild stress (UCMS) experiment was performed as described previously [31]. Mice were randomized into a control and UCMS group, and the UCMS model was established 1 week after acclimatization. Animals were exposed to mild unpredictable stresses of different types and time frames for 35 days, including food or water deprivation, a crowded environment, cage tilting, wet bedding, intermittent light, odor stimulation, electric shocks to the soles of the feet, noise, restraint, etc. Several different stresses were applied in the modeling process in a randomized order, so that the animals could not anticipate the stimuli. The behavioral tests were conducted 24 h after the end of modeling.

Behavioral tests

Open field test. Mice were individually placed in the center zone of a chamber (50 × 50 cm) with dim light for 5 min. Movement was tracked by a camera, which was positioned directly above the arena. The total distance of each mouse traveled was analyzed.

Tail suspension test. Mice that had been acclimatized to the test environment for 24 h were gently removed from the cages, and their tails were quickly secured with medical tape 2 cm from the tip without causing unnecessary pain or stress to the mice. During a total of 6 min of video recording, the immobile time in the last 4 min was recorded by referring previous literature [32]. After the recording, the mice were returned to the transition cage, and the apparatus was cleaned of urine and feces in a timely manner.

Forced swim test. The forced swim test was performed in cylinders (12 cm diameter and 25 cm height) filled with water (24 °C). Mice that had been acclimatized to the test environment for 24 h were gently taken out of the cage, grasped by the tail at a position between 1/3 and 2/3 of the length and slowly placed in the water. During 5 min of video recording, the time when the animals gave up struggling and remained still for the last 4 min was recorded. For each animal, the water was the temperature was brought up to 24 °C again before the experiment, and the cylinder was washed once with fresh water and refilled with water. At the end of the experiment, the mice were dried with paper towels.

Surgery and viral injection

To increase DCC expression, the viral LV-CaMKIIa-DIO-DCC-3XFlag-WPRE (titer: 1.50×10^{9} vector genome [v.g.]/mL, 0.3 μL) and rAAV-hSyn-CRE-WPRE-hGH-pA (titer: 5.18×10^{12} vector genome [v.g.]/mL, 0.1 μL) were mixed at a 3:1 ratio and injected into the bilateral mPFC of mice. A LV-CaMKIIa-DIO-3XFlag-WPRE (titer: 5.00×10^{7} vector genome [v.g.]/mL, 0.3 μL) virus was used in the control group. To label different types of neurons in the mPFC, the viruses AAV2/9-CaMKIIa-mcherry-WPRE-hGH-pA (titer: 5.29×10^{12} vector genome [v.g.]/mL, 0.2 μL) and AAV2/9-GAD67-mcherry-WPRE-hGH-pA (titer: 5.36×10^{12} vector genome [v.g.]/mL, 0.2 μL) were injected into the bilateral mPFC of mice. For chemical genetics experiments, the virus rAAV-CaMKIIa-hM4Di-EGFP-WPRE-hGH (titer: 2.75×10^{12} vector genome [v.g.]/mL, 0.2 μL) was injected into the bilateral mPFC, and the rAAV-CaMKIIa-EGFP-WPRE-hGH (titer: 5.00×10^{12} vector genome [v.g.]/mL, 0.2 μL) virus was used in the control group.

Before stereotaxic positioning, the mice were placed in a gas anesthesia machine and anesthetized rapidly with isoflurane (RWD, Shenzhen, China). Thereafter, using a calibrated glass microelectrode connected to an infusion pump (RWD), 200–300 nL (depending on the titer and expression) of the virus was injected into the mPFC (AP, +1.80 mm from bregma; ML, ±0.35 mm; DV, −2.4 mm from the brain surface) at a rate of 50 nL/min. To prohibit virus leakage, the electrode was left at the injection site for 15 min after the virus injection was completed.

Chemogenetic manipulation

For chemogenetic manipulation of mPFC neurons, C57BL/6 J mice were injected bilaterally into the mPFC with viral AAV-CaMKIIa-hM4Di-EGFP or viral AAV-CaMKIIa-EGFP. After 4 weeks infection, the mice were subjected to LH modeling, and the $CaMKII^{+}$ neurons of the mPFC was silenced by intraperitoneal injection of clozapine N-oxide (CNO) (3 mg/kg, Brain VTA) 30 min before modeling for 3 consecutive days. Behavioral tests were performed the day after modeling.

In vivo pharmacological methods

The mice were fixed on a brain stereotaxic apparatus (RWD) and, after leveling the mouse brain with the stereotaxic apparatus, a cannula (internal diameter 0.25 mm, RWD) was slowly inserted into the mPFC, with the cannula position determined using the brain atlas, and fixed with dental cement. The mice were allowed to recover for 2 weeks after surgery for cannula insertion before the experiments began. The drug-administration experiments were started 2 h after modeling and continued

every day for 3 consecutive days. The mice were maintained under anesthesia with a gas anesthesia machine, then the catheter cap was unscrewed to expose the drug delivery cannula. The inner injection tube was connected to a microsyringe via PE tubing, and the microsyringe was assembled with a microsyringe pump to aspirate the drug solution, which was injected into the mPFC at a flow rate of 100 nL/min with either calpeptin (0.5 μg/300 nL/day, Selleck) or artificial cerebrospinal fluid (300 nL/day). After the injection, the pressure was held for 5 min to allow the drug to fully diffuse, and administration was concluded by slowly removing the inner injection tube, reinserting the catheter cap and screwing it tightly closed. Behavioral tests were performed 24 h after the end of the modeling.

Electrophysiology

Mice were anesthetized with isoflurane and decapitated. The whole brain was rapidly removed and fixed in ice-cold oxygenated (95% O_2 and 5% CO_2) cutting solution (88 mM NaCl, 7 mM $MgCl_2$, 0.5 mM $CaCl_2$, 2.5 mM KCl, 1.25 mM NaH_2PO_4, 25 mM $NaHCO_3$, 75 mM sucrose). Coronal brain slices (300 μm thickness) were sectioned with a vibratome (VT1200S, Leica, Germany) and incubated in oxygenated artificial cerebrospinal fluid containing: 126 mM NaCl, 2.5 mM KCl, 1.25 mM NaH_2PO_4, 25 mM $NaHCO_3$, 2 mM $CaCl_2$, 2 mM $MgSO_4$, 10 mM glucose. Slices were allowed to recover at 32 °C for at least 1 h.

Whole-cell patch-clamp recordings were conducted on visually identified neurons under a fluorescence microscope (BX51WI, Olympus, Japan) equipped with a 403 Olympus water immersion lens and differential interference contrast optics. Slices were continuously superfused with artificial cerebrospinal fluid at 2–3 mL/min. Patch electrodes (4–5 MΩ) were pulled with a pipette puller (P2000; Sutter Instrument, USA) from borosilicate glass capillaries. Whole-cell recordings were obtained with an internal solution containing: 130 mM K-gluconate, 5 mM NaCl, 10 mM HEPES, 1 mM EGTA, 1 mM Na-GTP, 2 mM Mg-ATP. To assess the effects of NT-1 on neurons, whole-cell recordings were conducted following a 20-min incubation of the brain slices in 200 ng/mL of NT-1, during which NT-1 remained present in the bath solution. Electrophysiological recordings were acquired with a MultiClamp 700B amplifier (Axon-700B, MD, USA) and Clampex 10.6 software.

Immunofluorescence staining

Mice were anesthetized with isoflurane and sequentially perfused with saline and 4% PFA. Brains were incubated in PBS containing 30% sucrose until they sank to the bottom. Cryostat sections (40 μm) were collected (Leica, VT1200S) and incubated with blocking solution (PBS containing 5% goat serum and 0.5% Triton X-100) for 2 h at room temperature, then treated with primary antibodies, including anti-DCC (1:400, mouse, #515834, Santa Cruz), anti-c-Fos (1:1500, rabbit, #2250S, Cell Signaling Technology), anti-Flag (1:400, mouse, #66008-4-Ig, Proteintech), anti-NeuN (1:800, rabbit, #24307 T, Cell Signaling Technology) diluted with blocking solution for 48 h at 4 °C. The sections were washed three times with PBS before incubation with secondary antibodies (tagged with Alexa-Fluor 405, Alexa-Fluor 594, FITC; dilution 1:400; Zenbio) for 2 h at room temperature. Investigators were blind to group allocation when counting cells. The number of cells in the mPFC was recorded as the average of one set of brain slices. Analysis of average fluorescence intensity entailed the use of imaging software to measure the fluorescence intensity in the positive area of each brain section while employing standardized parameter settings. The average fluorescence intensity represented the mean fluorescence intensity value across a cohort of brain sections.

Western blotting

mPFC tissue was homogenized in lysis buffer (RIPA) (#0010, Solarbio) containing 1% PMSF (#P0100, Solarbio) on ice and subsequently centrifuged. Supernatants were transferred to a 2.5 mL tube, and proteins were separated using 10% SDS-PAGE gels (Tanon). The proteins were electrotransferred onto nitrocellulose membranes in ice-cold buffer (25 mM Tris HCl, 2 mM glycine, and 20% methanol), and the membranes were blocked with 5% nonfat milk powder dissolved in PBST and incubated overnight at 4 °C with antibodies. The following primary antibodies were used: anti-DCC (1:1000, #515834, Santa Cruz Biotechnology); anti-NT-1 (1:400, #20235-1-Ig, Proteintech); anti-GAPDH (1:1000, #200306-7E4, Zenbio), and anti-β-actin (1:1000, #200068-8F10, Zenbio). Horseradish peroxidase-conjugated goat anti-mouse and goat anti-rabbit secondary antibodies were purchased from Zenbio. Protein bands were visualized by chemiluminescence and quantified using ImageJ software.

Statistical analysis

All data presented in this work were obtained from experimental replicates, i.e., multiple animal cohorts from different litters, with at least three experimental repeats for each micrograph. GraphPad Prism 9 (GraphPad Software, Inc., USA) was used for statistical analyses and generating plots. Data are expressed as mean ± SEM and had normal distribution and homogeneity of variances. Student's t-test was used for statistical comparisons between two groups, and the one-way ANOVA test followed by Tukey test was used for comparisons among different experimental groups. Significance levels were expressed as * $p < 0.05$, ** $p < 0.01$, *** $p < 0.001$, and **** $p < 0.0001$.

RESULTS

Learned helplessness causes increased expression of DCC in the mPFC

Initially, we examined the expression of DCC and its ligand NT-1 in LH mice and control mice. The results showed that DCC and its ligand NT-1 were significantly up-regulated in the mPFC of mice 24 h after LH compared with those in control mice, but the levels of the two proteins had not changed in the mPFC 15 min and 3 h after LH (Fig. 1A–F). DCC in the mPFC was co-labelled with mature neurons using a mature neuronal marker, NeuN (Fig. 1G). To further clarify the specific neuron types, we performed co-labeling of DCC with tracer viruses from different neuronal promoters, and the results showed that DCC was highly expressed in $CaMKII^+$ neurons (86.3%) but not GABAergic neurons (9.9%) (Fig. 1H, I).

To clarify the association between behavioral despair and DCC, we classified the mice into stress-susceptible and stress-resilient groups according to the results of the behavioral tests in comparison to those of the control mice [33]. The results showed that DCC was significantly up-regulated in the mPFC of the stress-susceptible mice but not that of the stress-resilient mice compared with the control mice (Figures S1A-S1B). Finally, to confirm that the aberrant expression of DCC is universal in behavioral despair, we used UCMS to generate a well-established model that mimics several psychopathological dimensions of behavioral despair (Figure S1C). Western blotting (WB) analysis showed that DCC and NT-1 proteins were significantly increased in the mPFC of UCMS mice compared with that of control mice (Figures S1D-S1F). We next evaluated the changes to DCC expression in LPS-treated mice (Figure S1G). Our data showed that mice with LPS (2 mg/kg/day, *i.p.*) also had a significant increase in DCC and NT-1 levels in the mPFC (Figures S1H-S1J). These results indicate that DCC expression was up-regulated in $CaMKII^+$ neurons of the mPFC in male mice with behavioral despair.

DCC overexpression in the mPFC respectively induces and promotes behavioral despair in normal and LH-triggered male mice

To determine the roles DCC plays in behavioral despair, we used a DCC-overexpressing LV virus and control LV virus to observe the effect of DCC on behavioral despair. LV-CaMKIIa-DCC virus or control virus was bilaterally injected into the mPFC (Fig. 2A, B). Immunofluorescence staining showed that neurons were successfully transfected with the DCC-overexpression virus 3 weeks later (Fig. 2C). The WB results also verified the expression efficiency of the DCC-overexpression virus (Fig. 2D–F). The results of the open field experiment showed no difference in the total distance traveled among the groups, indicating that the voluntary movement ability of the mice was not affected (Fig. 2G). In the tail suspension test and forced swim test, LH mice given mPFC injections of LV-OECon had significantly longer immobility times than control mice injected with the LV-OECon virus. Control mice that received LV-OEDCC had significantly longer immobility times than those that received the LV-OECon virus. Importantly, LH mice injected with LV-OEDCC had significantly longer immobility times than LH mice injected with LV-OECon (Fig. 2H, I).

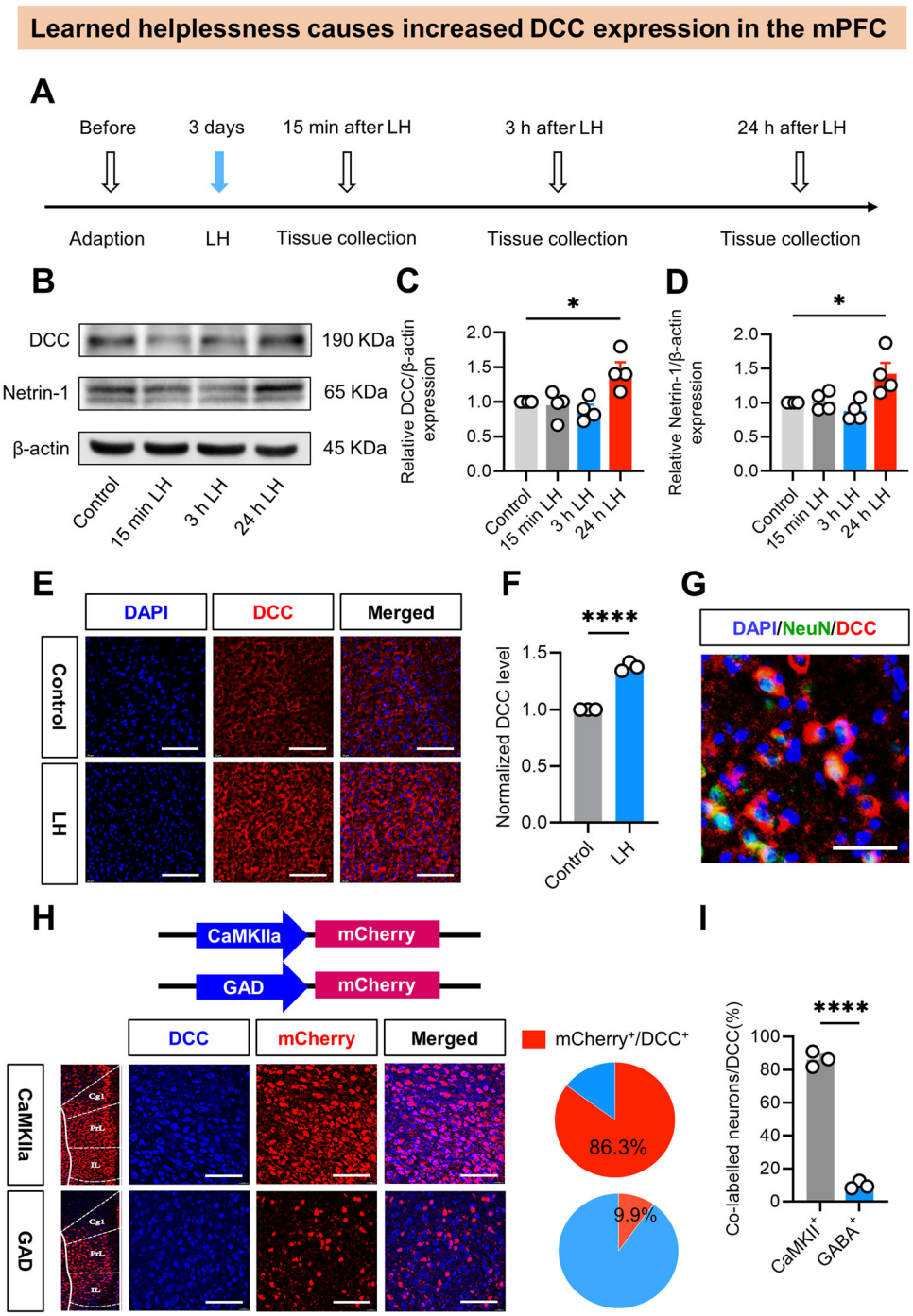

Fig. 1 Learned helplessness causes increased DCC expression in the mPFC. A Experimental paradigm for modeling learned helplessness in mice. **B–D** DCC and Netrin-1 expression in the mPFC of mice after LH establishment at different time points (n = 4 mice per group). **E, F** Representative images and quantification of DCC in the mPFC (n = 3 mice). Scale bars, 100 μm. **G** Representative images of the co-expression of NeuN and DCC in the mPFC. Scale bars, 100 μm. **H, I** Representative images and quantification of the co-expression of DCC and AAV-CaMKIIa-mCherry/AAV-GAD-mCherry expression in the mPFC (n = 3 mice). Scale bars, 100 μm. All data are mean ± SEM. * $p < 0.05$, **** $p < 0.0001$.

Neutralizing DCC activity alleviates behavioral despair in LH-triggered male mice

We further determined whether DCC played a role in modulating behavioral despair in LH mice. After LH modeling, the mice were randomly divided into DCC-neutralizing antibody (anti-DCC) and isotype control (inactivated anti-DCC) groups (Figures S2A-S2C). The open field test and movement trajectory graphs showed that there was no significant difference in the total distance travelled between the groups (Figures S2D and S2G). In the tail suspension and forced swim tests, LH mice infused with the isotype control had significantly increased immobility times than normal mice infused with the isotype control treatment. LH mice continuously infused with DCC-neutralizing antibodies showed a significantly shorter immobility time than LH mice infused with the isotype control treatments (Figures S2E-S2F). Our findings suggest that neutralizing DCC activity can alleviate behavioral despair in LH mice, but not in control mice.

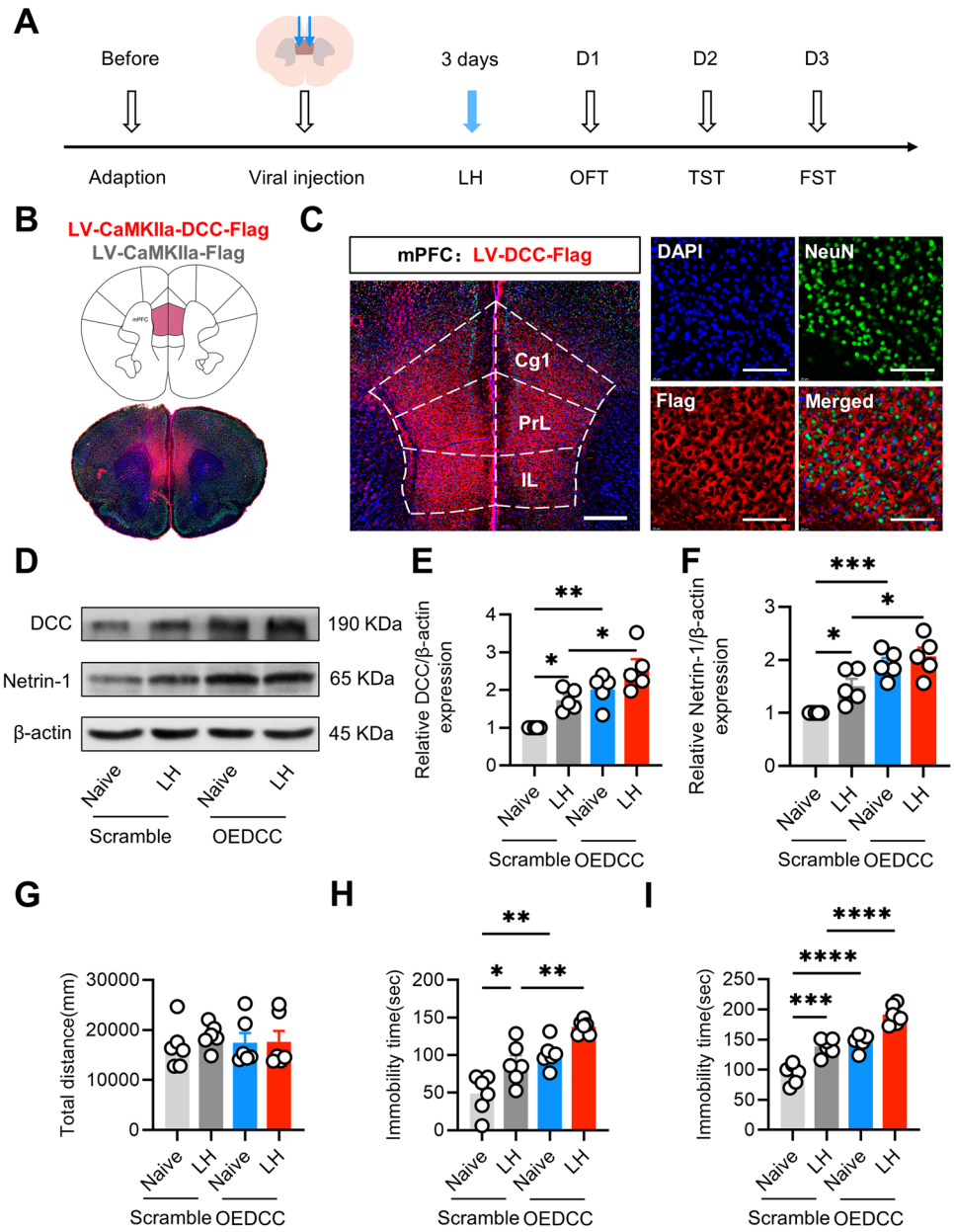

Fig. 2 DCC overexpression in the mPFC promotes behavioral despair in male mice. A Experimental paradigm for viral injection, modeling, and behavioral testing. **B** Schematic of viral infection and representative images of the expression of DCC in mPFC. **C** Representative images of LV-CaMKIIa-DCC-Flag expression in the mPFC of mice. Scale bars, 100 μm. **D**–**F** DCC and Netrin-1 in the mPFC after viral injection (n = 5 mice per group). **G** Total distance in the open field test (n = 6 mice per group). **H** Total immobility time in the tail suspension test (n = 6 mice per group). **I** Total immobility time in the forced swim test (n = 6 mice per group). All data are mean ± SEM. * $p < 0.05$, ** $p < 0.01$, *** $p < 0.001$, **** $p < 0.0001$.

Intraperitoneal injection of ketamine reduces the expression of DCC in the mPFC

To further assess the relationship between the expression level of DCC and behavioral despair, we examined DCC expression in LH mice that received ketamine (10 mg/kg), a fast-acting antidepressant that has been shown to have a long-lasting effect [34, 35]. The control group was given saline, and behavioral tests were performed 1 h later (Figure S3A). The results showed that ketamine-treated LH mice spent a significantly shorter time immobile in the forced swim test than the saline-treated LH mice, suggesting ketamine improved the behavioral despair (Figure S3B). WB results showed that the expression level of DCC in the mPFC of ketamine-injected LH mice was significantly reduced compared with that of the saline-injected mice (Figures S3C-S3D). These results suggest that DCC has the potential to be a new target for antidepressant therapy.

Overexcitation of CaMKII^{+} neurons in the mPFC participates in DCC expression

Impairment of neuronal function in the mPFC contributes to the onset of depression-like syndrome [36]. Thus, we examined how neuronal activity in the mPFC changed during LH modeling. First, we performed immunofluorescence staining of c-Fos and found significantly more c-Fos-positive neurons in the mPFC 1.5 h after LH modeling than in that of the control mice (Figures S4A-S4B). To further clarify the types of neuronal populations that were activated in this process, we co-labeled c-Fos with tracer viruses from different neuronal promoters. The results showed that mPFC

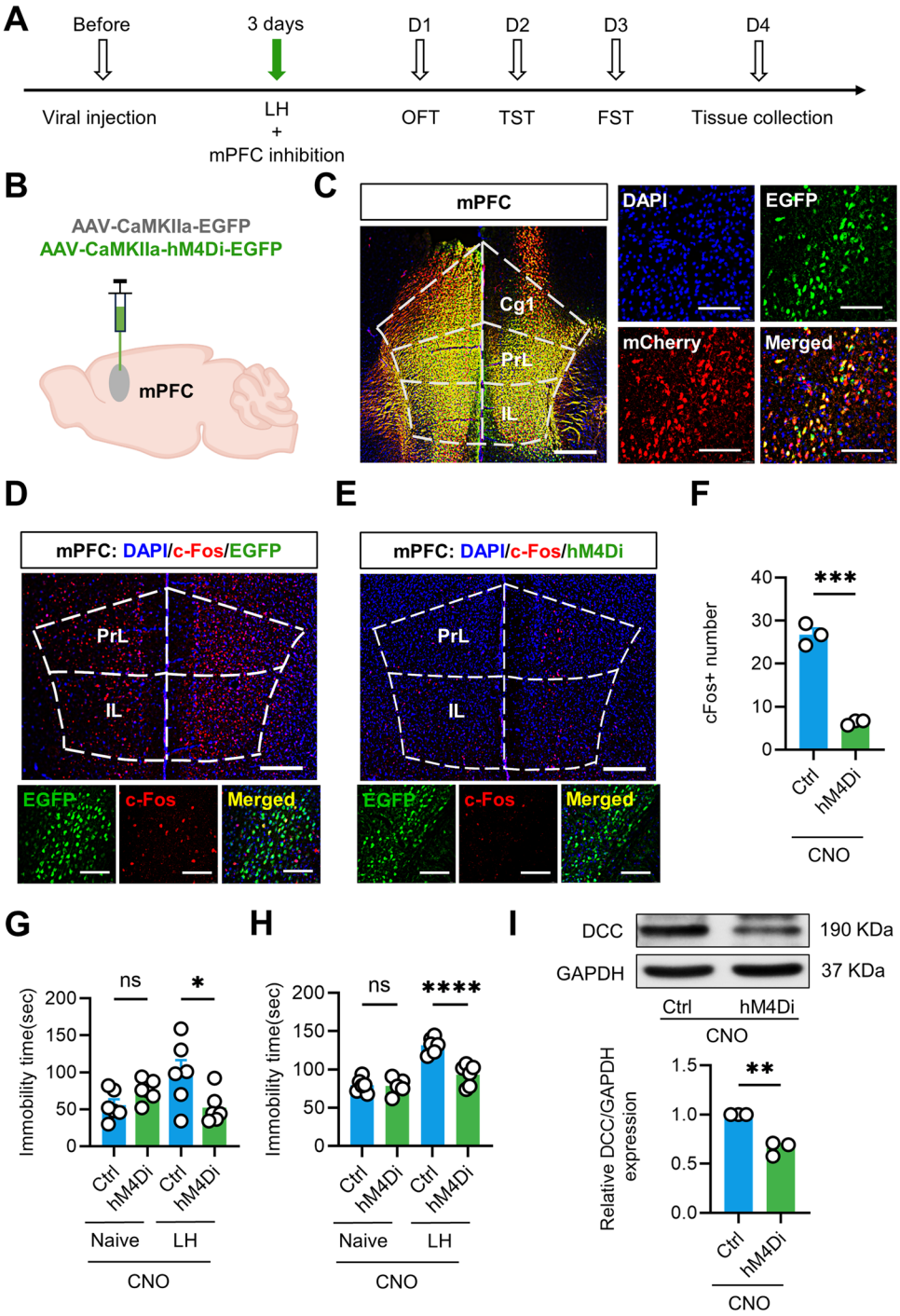

Fig. 3 Inhibition of mPFC CaMKII$^+$ neuronal activity before LH prevents the induction of behavioral despair in male mice. A Experimental paradigm for viral injection, modeling, and behavioral test. **B** Schematic of viral injection. **C** Representative images of viral expression in the mPFC. Scale bars, 100 μm. **D**–**F** Immunofluorescence representation and statistical results of the manipulation of CaMKII$^+$ neuronal activity by chemogenetics (n = 3 mice). Scale bars, 100 μm. **G** Total immobility time in the tail suspension test (n = 6 mice per group). **H** Total immobility time in the forced swim test (n = 6 mice per group). **I** DCC expression in the mPFC after viral injection (n = 3 mice per group). All data are mean ± SEM. * $p < 0.05$, ** $p < 0.01$, *** $p < 0.001$, **** $p < 0.0001$.

CaMKII$^+$ neurons were more highly activated in LH mice than normal mice (Figures S4C-S4E).

To confirm the effects of CaMKII$^+$ neurons on DCC expression, we used chemical genetics to inhibit the activity of mPFC CaMKII$^+$ neurons (Fig. 3A, B). Immunofluorescence co-staining showed that CaMKIIa-hM4Di-EGFP was strongly expressed in CaMKII$^+$ neurons (Fig. 3C) and that administration of CNO to reduce CaMKII$^+$ neuron activity decreased c-Fos expression, indicating the efficiency and reliability of inhibiting CaMKII$^+$ neuronal activity by chemical genetics (Fig. 3D–F). Behavioral tests with LH mice showed that, after chemogenetic inhibition of the activity of CaMKII$^+$ neurons, the mice did not have altered motor function, but there was an attenuation of behavioral despair and shortening of immobility times in the tail suspension test and forced swim test (Fig. 3G, H). By contrast, chemogenetic inhibition of the activity of CaMKII$^+$ neurons in normal mice did not affect their

behavioral despair (Fig. 3G, H). WB further showed that the expression level of DCC in the mPFC of the model group of mice expressing hM4Di was significantly reduced compared with that of the control group expressing EGFP (Fig. 3I). In conclusion, inhibition of mPFC CaMKII$^+$ neuron activity by chemical genetics before modeling blocked the development of behavioral despair and the expression of DCC in the mPFC of mice. These results suggest that overexcitation of CaMKII$^+$ neurons in the mPFC leads to the high expression of DCC, which may be an important cause of behavioral despair.

Calpain-SCOP/ERK is involved in pathological DCC expression

Calpain is activated by increased calcium levels and is necessary for neuronal activation processes and the regulation of neuronal function [37]. To further investigate the molecular mechanisms of impaired mPFC neuronal function involved in the development of behavioral despair, we performed LH modeling by intraperitoneally injecting mice for 3 days with the calpain inhibitor calpeptin or saline 2 h after LH modeling before subjecting the mice to the next set of behavioral experiments (Fig. 4A). The open field test showed that there was no significant difference in the total distance traveled among the groups (Fig. 4B). In the tail suspension and forced swim tests, calpeptin-treated LH mice had a significantly shorter immobility time compared with saline-treated LH mice, suggesting calpeptin lead to an improvement in behavioral despair. Control mice injected with either saline or calpeptin performed normally in the behavioral tests (Fig. 4C, D). WB results showed that DCC and its ligand NT-1 were significantly up-regulated in the mPFC of LH mice compared with that of control mice, while the expression levels of DCC and NT-1 were significantly lower in calpeptin-injected than saline-injected LH mice (Fig. 4E–G). These data suggest that calpain activation may induce the emergence of behavioral despair by modulating DCC expression.

As described previously, we first randomly grouped C57 mice and embedded a drug delivery cannula in the mPFC of each mouse (Fig. 4K). After 3–4 days of rest, the mice were subjected to LH modeling and were catheterized to receive a continuous infusion of calpeptin or artificial cerebrospinal fluid for 3 days, and then subjected to the next behavioral experiments. There was no significant difference in the total distance traveled among the groups in the open field test (Fig. 4H). In the tail suspension and forced swim tests, LH mice continuously infused with calpeptin had significantly shorter immobilization times than artificial cerebrospinal fluid -treated LH mice (Fig. 4I, J). Compared to artificial cerebrospinal fluid -treated LH mice, the LH mice given a continuous infusion of calpeptin levels exhibited significantly reduced DCC expression in the mPFC (Fig. 4L, M). These results suggest that calpain activation is an important cause of impaired neuronal function and high DCC expression in the mPFC.

Calpain degrades SCOP and activates ERK, which mediates protein synthesis and participates in changes to neuronal activity [38]. We next determined the downstream molecular mechanisms of calpain activation involved in the onset of behavioral despair using pharmacological methods. First, we examined the expression of p-ERK and SCOP in the mPFC of mice 15 min, 3 h, and 24 h after LH modeling. SCOP expression was down-regulated in the mPFC at the 15 min and 3 h time points after LH, and p-ERK was significantly up-regulated in the mPFC 15 min after LH. The expression levels of both proteins returned to baseline levels by 24 h after modeling (Fig. 5A–C), at which point, the expression level of DCC was increased. The above results indicate that the calpain-SCOP/ERK signaling pathway may be important for increasing the expression of DCC.

To further clarify that the calpain-SCOP/ERK signaling pathway is necessary for the high expression of DCC, we injected the ERK inhibitor SCH772984 or saline intraperitoneally 1 h prior to the LH modeling for a period of 3 days to induce the suppression of ERK activity and then performed behavioral tests (Fig. 5D). The open field test showed that there was no significant difference in the total distance traveled by the mice among the groups (Fig. 5E). In the tail suspension and forced swim tests, SCH772984-treated LH mice had significantly shorter immobility times than saline-treated LH mice. Control mice injected with either saline or SCH772984 performed normally in the behavioral tests (Fig. 5F, G). WB analysis showed that the phosphorylation level of ERK was significantly reduced in SCH772984-treated LH mice compared with saline-treated LH mice, confirming the efficacy of using SCH772984 to inhibit ERK activity (Fig. 5H, I). DCC and its ligand NT-1 were also significantly up-regulated in the mPFC of LH mice compared to that of control mice, and the expression levels of DCC and NT-1 were significantly lower in LH mice injected with SCH772984 than mice injected with saline and modeled with LH (Fig. 5J–L). The above findings suggest that calpain-SCOP/ERK is involved in pathological DCC expression.

Overexpression of DCC or NT-1 perfusion promotes excitation of mPFC CaMKII$^+$ neurons

We injected a stereotactic virus bilaterally into the mPFC of mice, and after 3 weeks of infection, the mice were tested behaviorally (Figures S5A-S5B). In the tail suspension test and forced swim test, mice injected with the DCC-overexpressing virus showed a significantly increased duration of immobility (Figures S5C-S5D). It has been reported in the literature that the dysregulation of neuronal excitatory homeostasis leads to the development of neuropsychiatric disorders such as depression-like syndrome [39]. To verify the effect of DCC on mPFC CaMKII$^+$ neuronal activity, we first performed immunofluorescence staining of c-Fos. This showed that the number of c-Fos-positive neurons in the mPFC of mice injected with the DCC-overexpression virus was significantly increased compared with that in mice injected with the control LV virus, suggesting that mPFC CaMKII$^+$ neuronal activity was significantly increased in mice after overexpression of DCC (Figures S5E-S5H).

We also used an ex vivo brain slice to compare the effects of NT-1 on the action potentials and spontaneous excitatory postsynaptic currents of pyramidal neurons in the mPFC (Fig. 6C). The results showed that perfusion of the mPFC with NT-1 increased the action potential firing frequency of pyramidal neurons compared with those in ACSF-treated slices (Fig. 6A, B). In addition, the frequency of spontaneous excitatory postsynaptic currents in pyramidal neurons in the mPFC was significantly increased after perfusion with NT-1 (*vs* control, $p < 0.05$, Fig. 6D–F). By contrast, there was no significant difference in amplitude between the groups (Fig. 6G, H). These data suggest that overexpression of DCC in the mPFC increases the excitability of CaMKII$^+$ neurons.

DISCUSSION

In this study, we observed a significant increase in DCC expression in the mPFC of male mice subjected to LH, LPS treatment, and UCMS. Moreover, overexpression of DCC in the mPFC induced and promoted behavioral despair in normal and LH mice, respectively. By contrast, neutralizing DCC activity alleviated behavioral despair in LH mice. Subsequent investigations revealed that the calpain-SCOP/ERK signaling pathway mediated the pathological expression of DCC through its influence on the excitation of CaMKII$^+$ neurons. The results of this study suggest that DCC is a key target in behavioral despair in male mice that might provide new strategies for treatment in the future.

mPFC DCC participates in the formation of behavioral despair in male mice

The mainstream view of the pathogenesis of depression-like syndrome includes the over-activation of the hypothalamic-

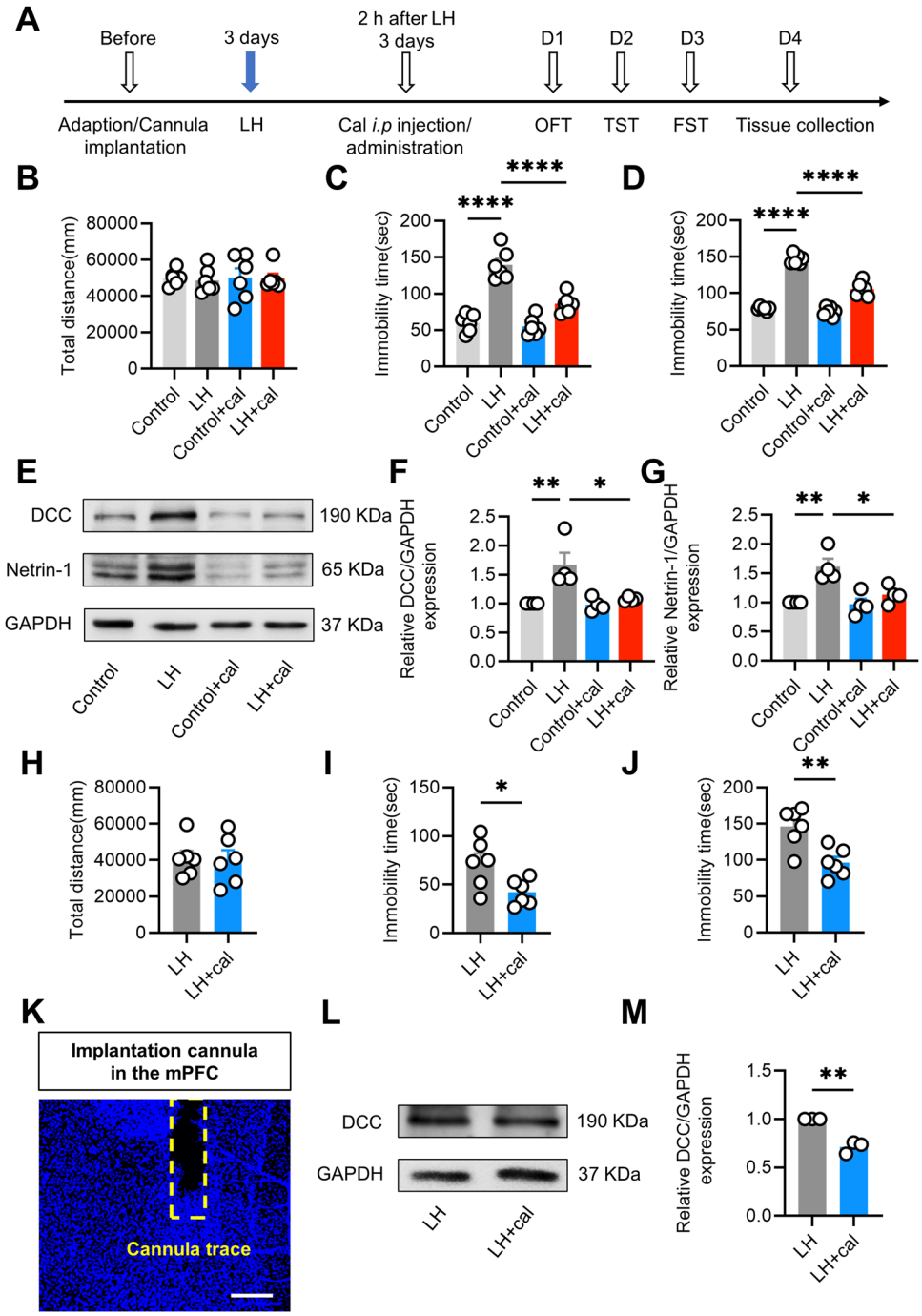

Fig. 4 Calpain inhibition alleviates behavioral despair in LH mice and inhibiting DCC expression in the mPFC. A Experimental paradigm for the experiments. **B** Total distance in the open field test (n = 6 mice per group). **C** Total immobility time in the tail suspension test (n = 6 mice per group). **D** Total immobility time in the forced swim test (n = 6 mice per group). **E**–**G** DCC and Netrin-1 in the mPFC of mice after calpain inhibition (n = 4 mice per group). **H** Total distance in the open field test (n = 6 mice per group). **I** Total immobility time in the tail suspension test (n = 6 mice per group). **J** Total immobility time in the forced swim test (n = 6 mice per group). **K** Confocal image of cannula site in the mPFC. Scale bar, 200 μm. **L**, **M** DCC in the mPFC of mice after calpain inhibition (n = 3 mice per group). All data are mean ± SEM. * $p < 0.05$, ** $p < 0.01$, **** $p < 0.0001$.

pituitary-adrenal axis [40], an imbalance in excitatory and inhibitory neurotransmission [41], and mitochondrial dysfunction [42]. Previous studies have shown that neuronal activity [43], energy metabolism [44], synaptic plasticity [45], and neural circuits are altered in the mPFC of animals with depression-like syndrome [46]. As a mediator and regulator of emotion control, the mPFC has often been the focus of research [47, 48]. Previous findings suggest that changes in neuronal activity in the mPFC control animal behavioral phenotypic outputs [49] such as the onset of behavioral despair. The present study, which was based on those research efforts, focused on the roles of DCC in the mPFC.

DCC and its ligand NT-1 participate in the activation of various signaling pathways that regulate cell migration, axon guidance, and neurogenesis, and they are considered critical regulatory factors in neurodevelopment [50]. At the same time, NT-1 and DCC are involved in pathological changes and contribute to the occurrence of diseases

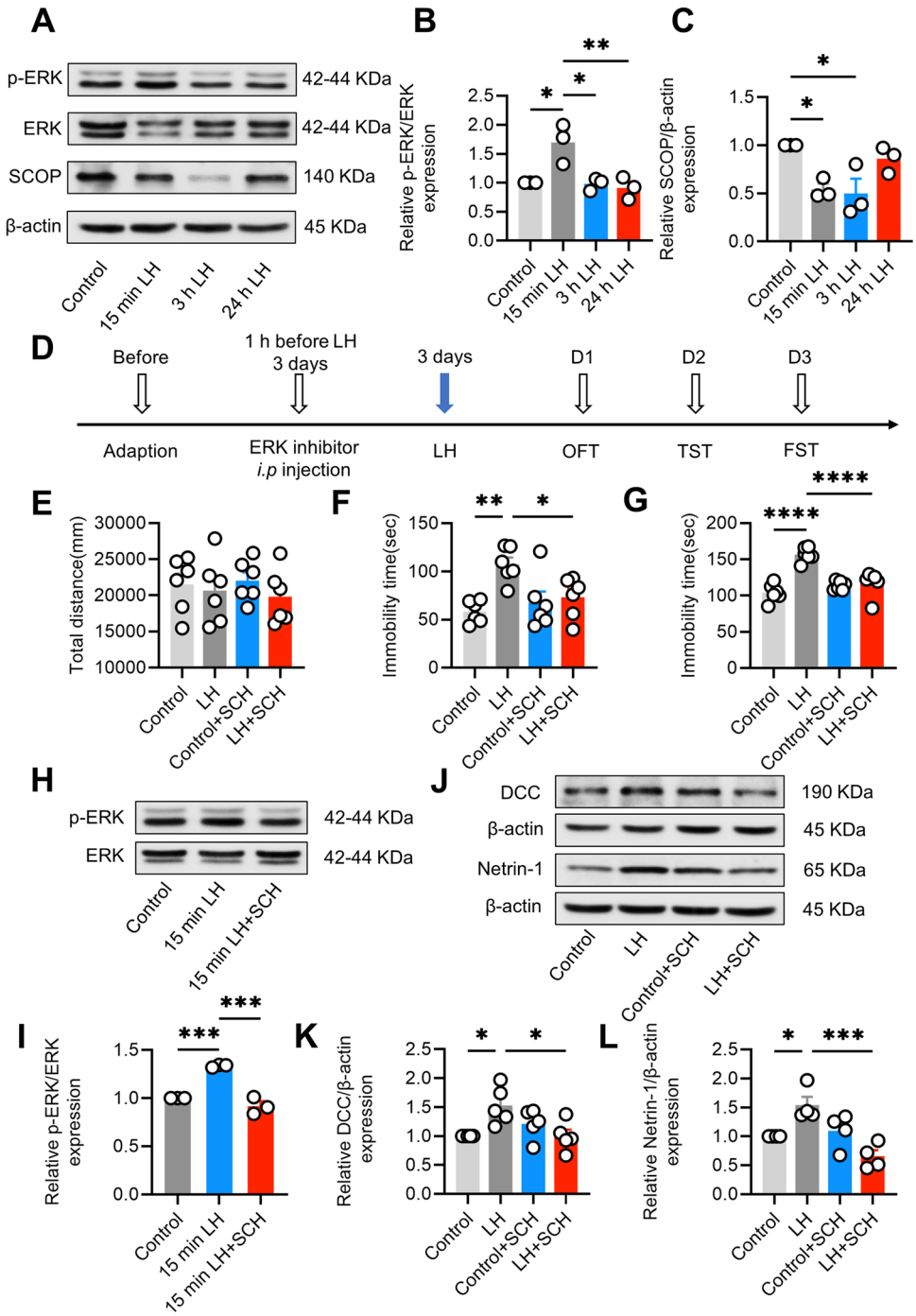

Fig. 5 ERK inhibition alleviates behavioral despair in LH mice and suppresses DCC expression in male mice. A–C DCC and Netrin-1 in the mPFC of mice after LH establishment at different time points (n = 3 mice per group). **D** Experimental paradigm for inhibitor administration, modeling, and behavioral test. **E** Total distance in the open field test (n = 6 mice per group). **F** Total immobility time in the tail suspension test (n = 6 mice per group). **G** Total immobility time in the forced swim test (n = 6 mice per group). **H, I** p-ERK protein in the mPFC after ERK inhibition (n = 3 mice per group). **J–L** DCC and Netrin-1 protein in the mPFC after ERK inhibition (n = 4 mice per group). All data are mean ± SEM. * $p < 0.05$, ** $p < 0.01$, *** $p < 0.001$, **** $p < 0.0001$.

such as Parkinson's disease [51, 52]. Clinical study has also shown a close association between genetic polymorphisms of NT-1 and DCC and the occurrence of depression [53]. Although DCC expression levels are known to be increased within the mPFC of depressed patients, it remains unclear whether DCC is a key player in mediating stress-induced behavioral despair or what the related mechanisms are. Sustained stress often leads to adaptive and abnormal responses in the brain, in which the dysregulation of neuronal function affects neuronal firing activity, which ultimately promotes the occurrence of mood disorders such as depression [54, 55]. In the present study, we applied several depressive stimuli, including UCMS, LPS, and LH, to investigate the roles DCC performs in behavioral despair. The psychological changes caused by pain and fear could also mimic post-traumatic stress disorder. We are committed to studying the mechanisms of traumatic psychological injury [56–58]. Therefore, we focused on the LH model in subsequent experiments. Like social-

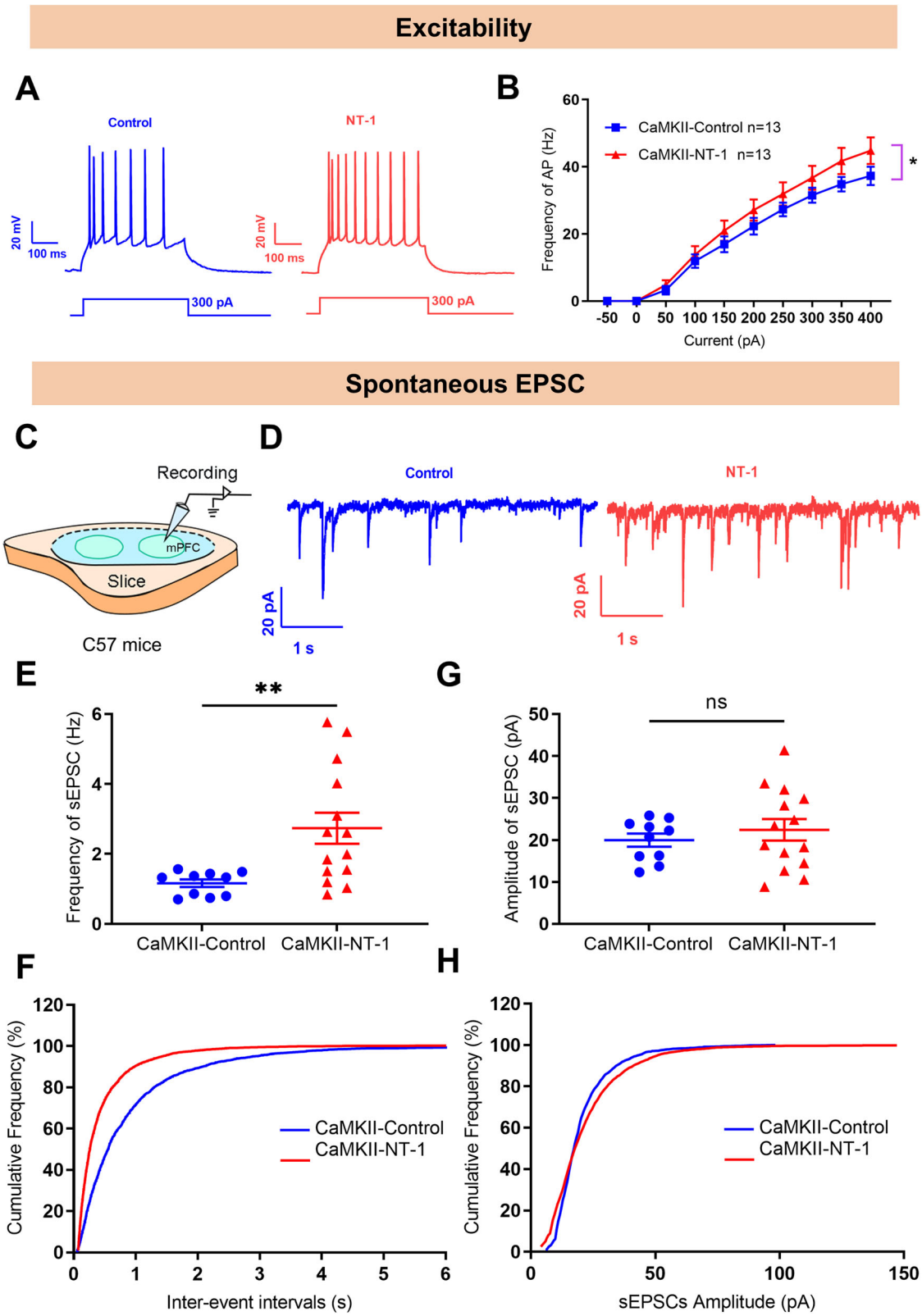

Fig. 6 Perfusion of NT-1 enhanced the neuronal excitability of CaMKII$^+$ neurons in the mPFC. A, **B** Sample traces and action potential data of CaMKII$^+$ neurons in the mPFC (n = 13 neurons per group). **C** Schematic diagram of electrophysiological recording of excitability of CaMKII$^+$ neurons in isolated brain slices. **D** Representative traces of the spontaneous excitatory postsynaptic current recorded from CaMKII$^+$ neurons in the mPFC. **E**, **F** Cumulative probability plots of the inter-event interval and average sEPSC frequency of CaMKII$^+$ neurons in the mPFC. **G**, **H** Cumulative probability plots and average sEPSC amplitude of CaMKII$^+$ neurons in the mPFC. All data are mean ± SEM. *$p < 0.05$, **$p < 0.01$.

defeat stress, UCMS, LPS, and LH stimulated DCC expression in the mPFC [59]. Importantly, we showed that DCC levels play a decisive role in behavioral despair with the following evidence. First, DCC was up-regulated in the mPFC of the stress-susceptible mice. Second, neutralizing DCC activity alleviated behavioral despair in LH mice. Third, the classical rapid anti-depressant drug ketamine also attenuated DCC expression. Finally, specific overexpression of DCC in $CaMKII^+$ neurons in the mPFC induced and promoted behavioral despair in normal and LH mice, respectively. These data together support the potential role of DCC in the pathogenesis and treatment of behavioral despair. However, the hippocampus, amygdala, and lateral habenula are also involved in the pathogenesis of behavioral despair [60]. The function of DCC in those brain regions still requires investigation. In addition to behavioral despair, anhedonia, a phenotype with the impairment of reward system is also a typical manifestation of depression-like syndrome [61]. The midbrain limbic system is a well-known reward system, involving the ventricular tegmental area and its projection target areas such as nucleus accumbens. Interestingly, DCC is also extensively expressed in those brain areas, which might explain its function in anhedonia.

Calpain-SCOP/ERK contributes to pathological DCC expression due to increased excitability of $CaMKII^+$ neurons

The mPFC consists of different neuronal populations, of which approximately 80% are excitatory pyramidal neurons, and the rest are inhibitory interneurons. Given the complexity of local microcircuit connections in the mPFC, it is reasonable to hypothesize that an imbalance between local excitatory and inhibitory microcircuits in the mPFC leads to the excitation of glutamatergic neurons, which in turn drives the onset and development of behavioral despair. It is therefore important to analyze how the different types of neurons interact and function in the depressed state. Our results revealed the abnormal activity patterns of $CaMKII^+$ neurons in the mPFC of despaired mice and indicated that DCC in the mPFC might be able to serve as a target for antidepressants.

Calcium ions play essential and important roles as indicators of neural activity in neuron growth, synaptic plasticity, the regulation of inflammatory responses, and learning memory [62]. Calpain is one member of a class of Ca^{2+}-dependent cysteine proteases that can be activated by high concentrations of Ca^{2+} and is essential for controlling the activation state of neurons. We have previously shown that calpain activation is a key step in the development of depression-like syndrome. SCOP is a pivotal molecule in the regulation of hippocampus-dependent long-term memory, and it is a degradation substrate of calpain. Study has shown that SCOP modulates ERK and has a negative correlation with ERK phosphorylation [63]. Given that calpain plays a crucial role in initiating neuronal excitability, we further examined the function of the calpain-SCOP/ERK signaling pathway in regulating DCC expression in the present study. We found that SCOP levels tended to decrease while the phosphorylation of ERK increased after LH. However, the changes were only temporary, and they returned to baseline 24 h later, retaining DCC at a high level of expression. As previously reported, the calpain-SCOP/ERK signaling pathway regulates new protein synthesis during synaptic activation [64]. Inhibition of glutamatergic neurons, calpain activity, and ERK phosphorylation during this process can attenuate DCC levels, indicating that calpain-SCOP/ERK signaling pathway activation probably contributes to pathological DCC expression. Interestingly, the decrease in SCOP expression and unaltered ERK phosphorylation 3 h after LH seems contradictory, indicating other suppressors might inhibit ERK phosphorylation.

NT-1/DCC expression leads to the excitation of $CaMKII^+$ neurons

It has been noted that chronic stress attenuates the claustrum (CLA)-mPFC excitatory loop, enhances the levels of the κ-opioid receptor (KOR) and its ligand dynorphin, and boosts excitatory neuronal activity in the mPFC. Earlier hybridization experiments showed that KOR is enriched in CLA excitatory neurons that project into the mPFC. KOR and its antagonist were shown to block chronic stress-induced depression-like syndrome. The ligand for DCC, NT-1 is also widely distributed in several brain regions, including the thalamus, amygdala, and hippocampus [65]. Given that the thalamus and cortex share neural connections, it is reasonable to speculate that NT-1, which is richly expressed in the thalamus, may be involved in behavioral despair via its regulation of neuronal plasticity in the mPFC.

Interestingly, DCC is expressed at low levels in the rodent brain [66] but is elevated in many neurological disorders. The above experiments demonstrated that excitatory $CAMKII^+$ neurons can activate the calpain-SCOP/ERK signaling pathway to increase DCC expression. This finding points towards a potential mechanism that regulates DCC levels in neurons. In our study, we also found that the overexpression of DCC or stimulation of excitatory $CAMKII^+$ neurons with NT-1 may be an important mechanism contributing to the reduction in the excitability threshold and development of behavioral despair in susceptible animals. In previous studies, we found that a single prolonged stressor that stimulated post-traumatic stress disorder also promoted hippocampal DCC expression. Overexpression of DCC activated the RAS-related C3 botulinum toxin substrate 1 (RAC1)-P21-activated kinase 1 (PAK1) pathway and disrupted long-term potentiation and learning memory [67, 68]. Therefore, further research is needed to determine whether DCC promotes RAC1-PAK1 signaling pathway activity to reduce the excitation threshold of neurons.

In our study, we employed chemogenetic inhibition of excitatory CAMKII-positive neurons in the LH region and found it effectively blocked the progression of behavioral despair. However, in a clinical setting, it is challenging to control stressors, making it difficult to implement strategies that involve inhibiting neuronal excitation. This poses a challenge for translating this approach into clinical applications. To control this microcircuit, we propose targeting the key molecule DCC and postulate that interventions for behavioral despair can be achieved using neutralizing antibodies against DCC. We believe that future research should focus more on DCC as a potential target for the development of antidepressant drugs.

Research perspectives and limitations of the study

One limitation of this study is that only male mice were included. Future experiments should explore whether similar behavioral phenotypes and underlying mechanisms exist in female mice. Another limitation of the study is that this study exclusively focused on elucidating how DCC impacts behavioral despair through its regulation of the function of $CaMKII^+$ neurons. However, it is worth noting that DCC is also expressed in GABAergic neurons. Therefore, the role of DCC in the function of GABAergic neurons in the mPFC, as well as whether it is involved in the regulation of behavioral despair, needs to be explored in depth.

CONCLUSION

In conclusion, our data indicate that LH triggers the excessive excitation of $CaMKII^+$ neurons and activation of calpain-SCOP/ERK signaling, which promotes DCC expression, and DCC is an important target for treatments to ameliorate LH-induced behavioral despair in male mice. This study has not only helped us to understand the pathogenesis of behavioral despair but also provided new intervention targets for the clinical treatment of depression.

DATA AVAILABILITY

Data will be made available based on reasonable request.

REFERENCES

1. Malhi GS, Mann JJ. Depression. Lancet. 2018;392:2299–312.
2. Moussavi S, Chatterji S, Verdes E, Tandon A, Patel V, Ustun B. Depression, chronic diseases, and decrements in health: results from the world health surveys. Lancet. 2007;370:851–8.
3. Ward J, Lyall LM, Bethlehem RAI, Ferguson A, Strawbridge RJ, Lyall DM, et al. Novel genome-wide associations for anhedonia, genetic correlation with psychiatric disorders, and polygenic association with brain structure. Transl Psychiatry. 2019;9:327.
4. Hammen C. Risk factors for depression: an autobiographical review. Annu Rev Clin Psychol. 2018;14:1–28.
5. Okbay A, Baselmans BML, De Neve J-E, Turley P, Nivard MG, Fontana MA, et al. Genetic variants associated with subjective well-being, depressive symptoms, and neuroticism identified through genome-wide analyses. Nat Genet. 2016;48:624–33.
6. Daly M, Robinson E. Depression and anxiety during COVID-19. Lancet. 2022;399:518.
7. Taquet M, Holmes EA, Harrison PJ. Depression and anxiety disorders during the COVID-19 pandemic: knowns and unknowns. Lancet. 2021;398:1665–6.
8. McCarron RM, Shapiro B, Rawles J, Luo J. Depression. Ann Intern Med. 2021;174:ITC65–ITC80.
9. Zhang Y, Zanos P, Jackson IL, Zhang X, Zhu X, Gould T, et al. Psychological stress enhances tumor growth and diminishes radiation response in preclinical model of lung cancer. Radiother Oncol. 2020;146:126–35.
10. Vosberg DE, Beaulé V, Torres-Berrío A, Cooke D, Chalupa A, Jaworska N, et al. Neural function in DCC mutation carriers with and without mirror movements. Ann Neurol. 2019;85:433–42.
11. Dailey-Krempel B, Martin AL, Jo H-N, Junge HJ, Chen Z. A tug of war between DCC and ROBO1 signaling during commissural axon guidance. Cell Rep. 2023;42:112455.
12. Manitt C, Eng C, Pokinko M, Ryan RT, Torres-Berrío A, Lopez JP, et al. dcc orchestrates the development of the prefrontal cortex during adolescence and is altered in psychiatric patients. Transl Psychiatry. 2013;3:e338.
13. Goldman JS, Ashour MA, Magdesian MH, Tritsch NX, Harris SN, Christofi N, et al. Netrin-1 promotes excitatory synaptogenesis between cortical neurons by initiating synapse assembly. J Neurosci. 2013;33:17278–89.
14. Díaz MM, Tsenkina Y, Arizanovska D, Mehlen P, Liebl DJ. DCC/netrin-1 regulates cell death in oligodendrocytes after brain injury. Cell Death Differ. 2023;30:397–406.
15. Sun J, Cong Q, Sun T, Xi S, Liu Y, Zeng R, et al. Prefrontal cortex-specific Dcc deletion induces schizophrenia-related behavioral phenotypes and fail to be rescued by olanzapine treatment. Eur J Pharmacol. 2023;956:175940.
16. Li H-J, Qu N, Hui L, Cai X, Zhang C-Y, Zhong B-L, et al. Further confirmation of netrin 1 receptor (DCC) as a depression risk gene via integrations of multi-omics data. Transl Psychiatry. 2020;10:98.
17. Zeng Y, Navarro P, Fernandez-Pujals AM, Hall LS, Clarke T-K, Thomson PA, et al. A combined pathway and regional heritability analysis indicates NETRIN1 pathway is associated with major depressive disorder. Biol Psychiatry. 2017;81:336–46.
18. He J-G, Zhou H-Y, Xue S-G, Lu J-J, Xu J-F, Zhou B, et al. Transcription factor TWIST1 integrates dendritic remodeling and chronic stress to promote depressive-like behaviors. Biol Psychiatry. 2021;89:615–26.
19. Torres-Berrío A, Morgunova A, Giroux M, Cuesta S, Nestler EJ, Flores C. miR-218 in adolescence predicts and mediates vulnerability to stress. Biol Psychiatry. 2021;89:911–9.
20. Fan J, Guo F, Mo R, Chen L-Y, Mo J-W, Lu C-L, et al. O-GlcNAc transferase in astrocytes modulates depression-related stress susceptibility through glutamatergic synaptic transmission. J Clin Invest. 2023;133:e160016.
21. Fan Z, Chang J, Liang Y, Zhu H, Zhang C, Zheng D, et al. Neural mechanism underlying depressive-like state associated with social status loss. Cell. 2023;186:560–76.e17.
22. Zhou T, Zhu H, Fan Z, Wang F, Chen Y, Liang H, et al. History of winning remodels thalamo-PFC circuit to reinforce social dominance. Science. 2017;357:162–8.
23. Wang Y-J, Zan G-Y, Xu C, Li X-P, Shu X, Yao S-Y, et al. The claustrum-prelimbic cortex circuit through dynorphin/κ-opioid receptor signaling underlies depression-like behaviors associated with social stress etiology. Nat Commun. 2023;14:7903.
24. Liu X, Li M, Chen Z, Yu Y, Shi H, Yu Y, et al. Mitochondrial calpain-1 activates NLRP3 inflammasome by cleaving ATP5A1 and inducing mitochondrial ROS in CVB3-induced myocarditis. Basic Res Cardiol. 2022;117:40.
25. Zhang M, Wang G, Peng T. Calpain-mediated mitochondrial damage: an emerging mechanism contributing to cardiac disease. Cells. 2021;10:2024.
26. Gao A, McCoy HM, Zaman V, Shields DC, Banik NL, Haque A. Calpain activation and progression of inflammatory cycles in Parkinson's disease. Front Biosci. 2022;27:20.
27. Mahaman YAR, Huang F, Kessete Afewerky H, Maibouge TMS, Ghose B, Wang X. Involvement of calpain in the neuropathogenesis of Alzheimer's disease. Med Res Rev. 2019;39:608–30.
28. Song Z, Shen F, Zhang Z, Wu S, Zhu G. Calpain inhibition ameliorates depression-like behaviors by reducing inflammation and promoting synaptic protein expression in the hippocampus. Neuropharmacology. 2020;174:108175.
29. Yang S-J, Song Z-J, Wang X-C, Zhang Z-R, Wu S-B, Zhu G-Q. Curculigoside facilitates fear extinction and prevents depression-like behaviors in a mouse learned helplessness model through increasing hippocampal BDNF. Acta Pharmacol Sin. 2019;40:1269–78.
30. Li W, Ali T, Zheng C, He K, Liu Z, Shah FA, et al. Anti-depressive-like behaviors of APN KO mice involve Trkb/BDNF signaling related neuroinflammatory changes. Mol Psychiatry. 2022;27:1047–58.
31. Shen F, Song Z, Xie P, Li L, Wang B, Peng D, et al. Polygonatum sibiricum polysaccharide prevents depression-like behaviors by reducing oxidative stress, inflammation, and cellular and synaptic damage. J Ethnopharmacol. 2021;275:114164.
32. Cao X, Li LP, Wang Q, Wu Q, Hu HH, Zhang M, et al. Astrocyte-derived ATP modulates depressive-like behaviors. Nat Med. 2013;19:773–7.
33. Si L, Xiao L, Xie Y, Xu H, Yuan G, Xu W, et al. Social isolation after chronic unpredictable mild stress perpetuates depressive-like behaviors, memory deficits and social withdrawal via inhibiting ERK/KEAP1/NRF2 signaling. J Affect Disord. 2023;324:576–88.
34. Anand A, Mathew SJ, Sanacora G, Murrough JW, Goes FS, Altinay M, et al. Ketamine versus ECT for nonpsychotic treatment-resistant major depression. N Engl J Med. 2023;388:2315–25.
35. Dwyer JB, Landeros-Weisenberger A, Johnson JA, Londono Tobon A, Flores JM, Nasir M, et al. Efficacy of intravenous ketamine in adolescent treatment-resistant depression: a randomized midazolam-controlled trial. Am J Psychiatry. 2021;178:352–62.
36. Kuang X-J, Zhang C-Y, Yan B-Y, Cai W-Z, Lu C-L, Xie L-J, et al. P2X2 receptors in pyramidal neurons are critical for regulating vulnerability to chronic stress. Theranostics. 2022;12:3703–18.
37. Baudry M. Calpain-1 and Calpain-2 in the brain: Dr. Jekill and Mr Hyde? Curr Neuropharmacol. 2019;17:823–9.
38. Chang Y, Huang Z, Hou F, Liu Y, Wang L, Wang Z, et al. Parvimonas micra activates the Ras/ERK/c-Fos pathway by upregulating miR-218-5p to promote colorectal cancer progression. J Exp Clin Cancer Res. 2023;42:13.
39. Shi M-M, Fan K-M, Qiao Y-N, Xu J-H, Qiu L-J, Li X, et al. Hippocampal μ-opioid receptors on GABAergic neurons mediate stress-induced impairment of memory retrieval. Mol Psychiatry. 2020;25:977–92.
40. Nikkheslat N, McLaughlin AP, Hastings C, Zajkowska Z, Nettis MA, Mariani N, et al. Childhood trauma, HPA axis activity and antidepressant response in patients with depression. Brain, Behav, Immun. 2020;87:229–37.
41. Luscher B, Maguire JL, Rudolph U, Sibille E. GABAA receptors as targets for treating affective and cognitive symptoms of depression. Trends Pharmacol Sci. 2023;44:586–600.
42. Cao X, Li L-P, Wang Q, Wu Q, Hu H-H, Zhang M, et al. Astrocyte-derived ATP modulates depressive-like behaviors. Nat Med. 2013;19:773–7.
43. Liu J, Mo J-W, Wang X, An Z, Zhang S, Zhang C-Y, et al. Astrocyte dysfunction drives abnormal resting-state functional connectivity in depression. Sci Adv. 2022;8:eabo2098.
44. Song X, Chen X, Yuksel C, Yuan J, Pizzagalli DA, Forester B, et al. Bioenergetics and abnormal functional connectivity in psychotic disorders. Mol Psychiatry. 2021;26:2483–92.
45. Price RB, Duman R. Neuroplasticity in cognitive and psychological mechanisms of depression: an integrative model. Mol Psychiatry. 2020;25:530–43.
46. Li Y-F. A hypothesis of monoamine (5-HT) - Glutamate/GABA long neural circuit: aiming for fast-onset antidepressant discovery. Pharmacol Ther. 2020;208:107494.
47. Lei Y, Wang J, Wang D, Li C, Liu B, Fang X, et al. SIRT1 in forebrain excitatory neurons produces sexually dimorphic effects on depression-related behaviors and modulates neuronal excitability and synaptic transmission in the medial prefrontal cortex. Mol Psychiatry. 2020;25:1094–111.
48. Lin S, Huang L, Luo Z-C, Li X, Jin S-Y, Du Z-J, et al. The ATP level in the medial prefrontal cortex regulates depressive-like behavior via the medial prefrontal cortex-lateral habenula pathway. Biol Psychiatry. 2022;92:179–92.
49. Li C, Liu B, Xu J, Jing B, Guo L, Wang L, et al. Phloretin decreases microglia-mediated synaptic engulfment to prevent chronic mild stress-induced depression-like behaviors in the mPFC. Theranostics. 2023;13:955–72.
50. Dun X-P, Parkinson DB. Role of Netrin-1 signaling in nerve regeneration. Int J Mol Sci. 2017;18:491.
51. Stone TW, Darlington LG, Forrest CM. Dependence receptor involvement in subtilisin-induced long-term depression and in long-term potentiation. Neuroscience. 2016;336:49–62.

52. Horn KE, Glasgow SD, Gobert D, Bull S-J, Luk T, Girgis J, et al. DCC expression by neurons regulates synaptic plasticity in the adult brain. Cell Rep. 2013;3:173–85.
53. Arnau-Soler A, Macdonald-Dunlop E, Adams MJ, Clarke T-K, MacIntyre DJ, Milburn K, et al. Genome-wide by environment interaction studies of depressive symptoms and psychosocial stress in UK Biobank and Generation Scotland. Transl Psychiatry. 2019;9:14.
54. Li Y, Fan C, Wang L, Lan T, Gao R, Wang W, et al. MicroRNA-26a-3p rescues depression-like behaviors in male rats via preventing hippocampal neuronal anomalies. J Clin Invest. 2021;131:e148853.
55. Tunc-Ozcan E, Peng C-Y, Zhu Y, Dunlop SR, Contractor A, Kessler JA. Activating newborn neurons suppresses depression and anxiety-like behaviors. Nat Commun. 2019;10:3768.
56. Wang J, Gao F, Cui S, Yang S, Gao F, Wang X, et al. Utility of 7,8-dihydroxyflavone in preventing astrocytic and synaptic deficits in the hippocampus elicited by PTSD. Pharmacol Res. 2022;176:106079.
57. Gao F, Wang J, Yang S, Ji M, Zhu G. Fear extinction induced by activation of PKA ameliorates anxiety-like behavior in PTSD mice. Neuropharmacology. 2023;222:109306.
58. Ji M, Zhang Z, Gao F, Yang S, Wang J, Wang X, et al. Curculigoside rescues hippocampal synaptic deficits elicited by PTSD through activating cAMP-PKA signaling. Phytother Res. 2023;37:759–73.
59. Torres-Berrío A, Lopez JP, Bagot RC, Nouel D, Dal Bo G, Cuesta S, et al. DCC confers susceptibility to depression-like behaviors in humans and mice and is regulated by miR-218. Biol Psychiatry. 2017;81:306–15.
60. Cui Y, Yang Y, Ni Z, Dong Y, Cai G, Foncelle A, et al. Astroglial Kir4.1 in the lateral habenula drives neuronal bursts in depression. Nature. 2018;554:323–7.
61. von Mücke-Heim I-A, Urbina-Treviño L, Bordes J, Ries C, Schmidt MV, Deussing JM. Introducing a depression-like syndrome for translational neuropsychiatry: a plea for taxonomical validity and improved comparability between humans and mice. Mol Psychiatry. 2022;28:329–40.
62. Inglebert Y, Aljadeff J, Brunel N, Debanne D. Synaptic plasticity rules with physiological calcium levels. Proc Natl Acad Sci USA. 2020;117:33639–48.
63. Shimizu K, Kobayashi Y, Nakatsuji E, Yamazaki M, Shimba S, Sakimura K, et al. SCOP/PHLPP1β mediates circadian regulation of long-term recognition memory. Nat Commun. 2016;7:12926.
64. Zhu G, Liu Y, Wang Y, Bi X, Baudry M. Different patterns of electrical activity lead to long-term potentiation by activating different intracellular pathways. J Neurosci. 2015;35:621–33.
65. Ullah R, Shen Y, Zhou Y-D, Fu J. Perinatal metabolic inflammation in the hypothalamus impairs the development of homeostatic feeding circuitry. Metabolism. 2023;147:155677.
66. Torres-Berrío A, Hernandez G, Nestler EJ, Flores C. The Netrin-1/DCC guidance cue pathway as a molecular target in depression: translational evidence. Biol Psychiatry. 2020;88:611–24.
67. Hu J, Li H, Wang X, Cheng H, Zhu G, Yang S. Novel mechanisms of Anshen Dingzhi prescription against PTSD: inhibiting DCC to modulate synaptic function and inflammatory responses. J Ethnopharmacol. 2024;333:118425.
68. Yang S, Hu J, Chen Y, Zhang Z, Wang J, Zhu G. DCC, a potential target for controlling fear memory extinction and hippocampal LTP in male mice receiving single prolonged stress. Neurobiol Stress. 2024;32:100666.

AUTHOR CONTRIBUTIONS

PC, MC and GQZ designed the study and wrote the manuscript; PC, KKD, DKC, CY, JW and SJY conducted the study and did the statistical analysis.

FUNDING

This research was supported by Research Funds of Center for Xin'an Medicine and Modernization of Traditional Chinese Medicine of IHM (2023CXMMTCM013), Scientific Research Program of Anhui Provincial Department of Education (2024AH040137, 2024AH051044), Excellent Funding for Academic and Scientific Research Activities for Academic and Technological Leaders in Anhui Province (2022D317), Chinese Medicine Prevention and Treatment of Mental Illness Research Team (2024zyky02) and The Open Fund of High-level Key Discipline of Basic Theory of TCM of the State Administration of Traditional Chinese Medicine, Anhui University of Chinese Medicine (ZYJCLLZD-04).

ETHICS APPROVAL AND CONSENT TO PARTICIPATE

All animal experiments in this study were complied with National Institutes of Health (NIH) guidelines for the Care and Use of Laboratory Animals and approved by the Animal Ethics Committee of Anhui University of Chinese Medicine (AHUCM-mouse-2022014).

COMPETING INTERESTS

The authors declare no competing interests.

ADDITIONAL INFORMATION

Supplementary information The online version contains supplementary material available at https://doi.org/10.1038/s41398-025-03266-x.

Correspondence and requests for materials should be addressed to Ming Chen or Guoqi Zhu.